Received May 4, 2018, accepted June 8, 2018, date of publication June 15, 2018, date of current version July 25, 2018.

Digital Object Identifier 10.1109/ACCESS.2018.2847641

Set-Point Tracking and Multi-Objective Optimization-Based PID Control for the Goethite Process

XIAOJUN ZHOU, JIAJIA ZHOU, CHUNHUA YANG, AND WEIHUA GUI

School of Information Science and Engineering, Central South University, Changsha 410083, China

Corresponding author: Xiaojun Zhou (michael.x.zhou@csu.edu.cn)

This work was supported in part by the National Natural Science Foundation of China under Grant 61503416, Grant 61533021, and Grant 61725306, in part by the 111 Project under Grant B17048, in part by the Innovation-Driven Plan in Central South University under Grant 2018CX012, in part by the Foundation for Innovative Research Groups of the National Natural Science Foundation of China under Grant 61621062, in part by the Hunan Provincial Natural Science Foundation of China under Grant 2018JJ3683, and in part by the Fundamental Research Funds for the Central Universities of Central South University under Grant 2017zzts492.

ABSTRACT The goethite process is complicated since its chemical reactions interact with each other, making its control and optimization in industrial production difficult. The goal of the goethite process is to make the outlet ion concentration satisfy the technical requirements with minimal process consumption. To simplify the difficulties of optimization in the goethite process, an optimization method based on a set-point tracking strategy is proposed. The set-point tracking strategy is used to transform the complex state constraints into an additional objective. Therefore, the single optimization control problem for the goethite process is transformed into a bi-objective optimization control problem. Furthermore, PID controllers are adopted to control the addition amounts of zinc oxide and oxygen in the goethite process. The optimal parameters of the PID controllers are obtained via a multi-objective state transition algorithm (MOSTA). The performance of MOSTA is verified by several benchmark test functions with performance matrices. The control performance reveals that the proposed method is an effective way to control the process and can not only reduce the zinc oxide and oxygen addition amounts compared with manual operation and traditional PID control but also reject disturbances. The proposed method can satisfy the industrial requirements with less energy consumption.

INDEX TERMS Goethite process, multi-objective optimization, PID control, set-point tracking, state transition algorithm.

I. INTRODUCTION

As one of the most important metals, zinc is used in many industry fields, playing an important role in the battery, mechanical and chemical industries. Currently, hydrometallurgical extraction is the major approach to smelting zinc [1]. In the zinc hydrometallurgy process, iron ions must be removed from the leaching solution to enhance the efficiency of zinc electrolysis and improve the quality of the zinc product [2]. At present, the dissolved iron can be precipitated in the form of jarosite [3], hematite [4], and goethite [5], all of which are widely utilized in many smelting factories. Compared with other forms of iron precipitate, the goethite precipitate has many advantages. It contains higher concentrations of iron and larger crystal sizes, which can be utilized to smelt steel and bring better economic returns [6], [7]. Therefore, goethite precipitation has always been considered the best way to remove iron ions.

In the goethite process, oxygen is added to the zinc sulfate solution, and the ferrous iron is oxidized into ferric iron. Then, the ferric iron is hydrolysed to form the goethite polymer precipitate. There are three major chemical reactions involved in the formulation of the goethite precipitate that can be simply described by the following chemical equations [8]. A schematic diagram of the reactions in the goethite process is shown in Fig. 1.

$$\text{Oxidation reaction}: 4Fe^{2+} + 4H^{+} + O_2 \rightarrow 4Fe^{3+} + 2H_2O \quad (1)$$

$$\text{Hydrolysis reaction}: Fe^{3+} + 2H_2O \rightarrow FeOOH + 3H^{+} \quad (2)$$

$$\text{Neutralization reaction}: 2H^{+} + ZnO \rightarrow Zn^{2+} + H_2O \quad (3)$$

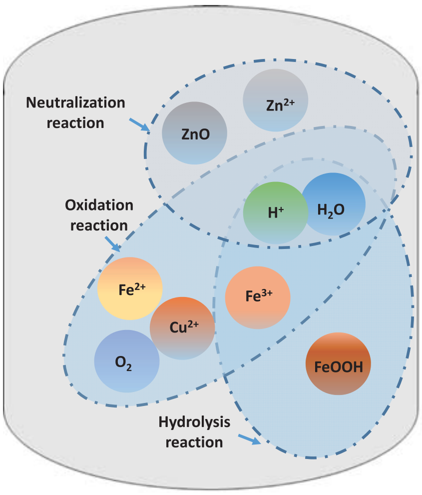

FIGURE 1. The schematic diagram of reactions in goethite process.

These chemical reactions are sensitive to the pH value [10]. If the pH is too high, other ions present in the zinc sulfate solution, such as $Cu(OH)_2$, will form precipitates. However, if the pH value is too low, the iron precipitate will redissolve, which will impede the process of iron ion removal. Therefore, zinc oxide powder is added to the zinc solution to keep the pH in equilibrium during the goethite process. The chemical equations mentioned in (1) – (3) reveal that the goethite process is complicated and that these reactions interact with each other. Thus, the process is difficult to control and must be optimized for industrial production. In industrial practice, manual operators adjust the amount of O_2 and ZnO added to control the ion concentration and pH value. The control objective of the goethite process is to satisfy the technical requirements with minimal consumption. However, it is difficult to take into account technical requirements and minimal consumption simultaneously.

There have been several previous achievements regarding the goethite process. In [9], Xie *et al.* investigated the optimal setting model of reactor outlet ferrous iron concentration and utilized the control parameterization method to solve the optimization problem for the iron precipitate production process. Numerical simulations showed that both the formation conditions of the goethite precipitate and the stability of the production process were satisfied by this approach. In [6], a dynamic model based on the rate-controlling step of the goethite process was established. In addition, an optimal control method was proposed that not only included presetting the descent gradient of the outlet ferrous ion concentration but also included optimal control of oxygen and zinc oxide. Industrial experiments showed that the average oxygen and zinc oxide consumptions were decreased compared to manual control. All of the previous studies provide theoretical fundamentals and inspiration for control of the goethite process. To the best of the authors' knowledge, all previous studies used the ion concentration requirements as constraints, which may have increased the difficulty of further optimization.

During the goethite process, the concentrations of outlet ferrous iron, ferric iron, and hydrogen ions need to be within a certain range. Thus, the state variables in the goethite process consist of the concentration of the outlet ions mentioned above. Considering the difficulty of state constraints when solving the optimization control problem for the goethite process, inspired the approach of tackling the input constraint in [12], a new optimization method based on a set-point tracking strategy is proposed. First, proper ion concentration set-points should be found with a reasonable approach. Then, the outlet ion concentrations are supposed to track the set-points such that the technical requirements of the outlet ion concentrations are naturally satisfied. Therefore, the state constraints of the outlet ion concentrations are transformed into an additional objective, and the optimization control problem for the goethite process is transformed into a bi-objective optimization problem. The first objective is to minimize energy consumption, and the other is to minimize the error between the outlet ion concentrations and the set-points. Here we adopt PID controllers since they are the most widely used controllers in industrial control and have great set-point tracking performance. However, the parameters of PID controllers have a significant influence on the control performance. Thus, to find optimal parameters, a new multi-objective optimization algorithm, named the multi-objective state transition algorithm (MOSTA), is proposed to solve the PID controller parameter tuning problem for the goethite process. For the purpose of verifying the advantages of optimization modelling methods based on set-point tracking strategies, several comparison experiments are conducted using multi-objective optimization control, single-objective optimization control, and manual control. The results indicate that multi-objective optimization control modeling based on set-point tracking strategies can ensure that outlet ion concentrations satisfy the technical requirements. Moreover, the outlet ion concentrations fluctuate less, which can provide smoother inlet ion concentrations for the next subprocess.

The major contributions and novelties in this paper are briefly summarized as follows. (i) A new optimization modelling method based on a set-point tracking strategy is proposed to address the state constraints in the optimization control problem for the goethite process. (ii) PID controllers are adopted to control the addition amount of zinc oxide and oxygen in the goethite process. Furthermore, the addition amount of zinc oxide and oxygen can be used to control the concentration of outlet ions. (iii) A multi-objective state transition algorithm is proposed to obtain the optimal parameters for the PID controllers. In addition, good performance is verified by several benchmark test functions using performance matrices. (iv) The effectiveness of the proposed method is presented by comparing the simulation results. The parameters of the PID controllers obtained by the proposed method can keep

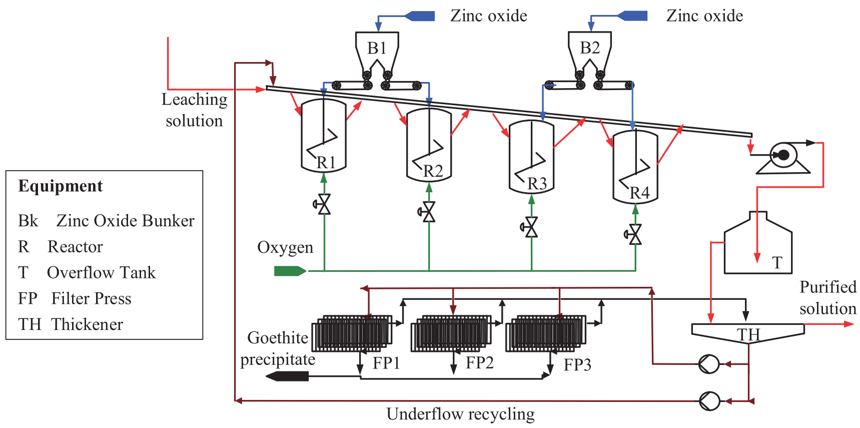

FIGURE 2. The schematic diagram of the goethite process.

TABLE 1. The desired specifications of the effluent in the goethite process.

Parameter	Unit	#1 Effluent	#2 Effluent	#3 Effluent	#4 Effluent
pH	–	2.7–3.5	2.7–3.5	2.7–3.5	2.7–3.5
Fe^{3+}	g/L	≤ 2	≤ 2	≤ 2	≤ 2
Fe^{2+}	g/L	6–8	2.5–5	1–2	0.3–0.8

TABLE 2. The oxygen and ferrous iron concentration in four reactors (unit: mmol/L).

Parameter	#1 Effluent	#2 Effluent	#3 Effluent	#4 Effluent
$C_{Fe^{2+}}$	107.4-214.9	53.7-107.4	17.9-71.6	3.6-35.8
C_{O_2}	3.8-6.4	13.9-15.0	9.6-10.4	5.0-8.7

ion concentrations steady and provide disturbance rejection performance.

II. ANALYSIS OF THE GOETHITE PRECIPITATION PROCESS

The goethite process is a significant part of the atmosphere direct leaching of zinc concentrates. The simplified schematic of the process is shown in Fig. 2. One can observe that the entire process consists of four large stirred tank reactors, each with a volume of approximately 300 m^3, and a thickener, which is used to divide the outlet solution of the fourth reactor # 4 into solid and liquid. Zinc solution, together with the returned underflow solution from the thickener, flows into the first reactor #1. Then, zinc solution overflows from the first reactor # 1 to the other three reactors in series with the first one [2]. The zinc oxide and oxygen are fed into the reactors to ensure the occurrence of chemical reactions and ensure the pH equilibrium of the solution. In actual industrial production processes, the quantity of the added zinc oxide is controlled by an electronic belt weigh feeder under manual control, which depends on the operators' experience and may lead to fluctuations in the control result and energy wastage. Therefore, it is important and necessary to design an optimal control law for the addition of oxygen and zinc oxide to obtain a satisfactory control performance with minimal process consumption. The ideal technical requirements of the effluent from reactor #1 to reactor #4 and the compositions of the influent flowing into reactor #1 to reactor #4 are shown in Table 1 and Table 2.

A. MODELLING OF THE GOETHITE PROCESS

In this section, based on the theory of first order chemical reaction kinetics, the model of the goethite process is established. This section includes two aspects: analysis of the chemical reaction and construction of the optimization problem for the goethite process. We make the following assumptions in analysing the goethite process:

i. The temperature and agitation rate in each reactor are assumed to be constant.
ii. In practice, the flow rate of the returned underflow and influent are controllable. Therefore, they are assumed to be constants.
iii. Because the pipes between the reactors are relatively short, any chemical reaction that might occur between two reactors is ignored [10].

1) ANALYSIS OF CHEMICAL REACTIONS IN THE GOETHITE PROCESS

In the goethite process, the chemical reactions occurring in the reactors are given in reactions (1) - (3). The outlet concentrations of ferrous ions, ferric ions and hydrogen ions are denoted by $c^i = [c_1^i, c_2^i, c_3^i]$, where i denotes reactor # i. In [6], the historical measurement data of ferrous iron and oxygen concentrations were obtained from a zinc hydrometallurgy plant with four reactors, which are shown in Table 2. The addition rate of oxygen and zinc oxide is denoted as $u^i = [u_1^i, u_2^i]$. In the oxidation reaction, copper is considered a catalyst, and the oxidation reaction in (1) can be divided into two sub-step reactions:

$$\mathrm{Fe}^{2+} + \mathrm{Cu}^{2+} \rightarrow \mathrm{Fe}^{3+} + \mathrm{Cu}^{+}, \tag{4-a}$$

$$4\mathrm{Cu}^{+} + \mathrm{O}_2 + 4\mathrm{H}^{+} \rightarrow 4\mathrm{Cu}^{2+} + 2\mathrm{H}_2\mathrm{O}. \tag{4-b}$$

According to the theory of the reaction rate control step, the reaction rate relies on the concentration of the reactant, and the overall reaction rate is determined by the lowest rate in the sub-step reaction. In reactor # 1, the concentration of ferrous iron is much higher than that of oxygen, as shown in Table 2. Thus the reaction rate of the first sub-step reaction is much higher than that of the second one. Furthermore, the oxidation reaction rate is approximately equal to the rate of the second sub-step reaction in reactor # 1. In contrast, in reactors # 2, # 3 and # 4, The ratio of ferrous ion concentration to oxygen concentration is comparable to that of stoichiometric coefficient of chemical reaction in oxidation reaction. Thus the oxidation reaction rate in reactors # 2, # 3 and # 4 is controlled by (1). The oxidation rate v_1^i of reactor #i can be described as follows:

$$v_1^i = \begin{cases} k_1^i(1+\eta^i C^i_{\mathrm{Cu}^{2+}})(C^i_{\mathrm{O}_2})^{\beta}(c_3^i)^{\gamma} & i = 1, \\ k_1^i(1+\eta^i C^i_{\mathrm{Cu}^{2+}})(c_1^i)^{\alpha}(C^i_{\mathrm{O}_2})^{\beta}(c_3^i)^{\gamma} & i = 2, 3, 4, \end{cases} \tag{5}$$

where k_1^i and η^i are the rate constant and the catalytic action coefficient in reactor # i, respectively. $C^i_{Cu^{2+}}$ and $C^i_{O_2}$ are the concentrations of Cu^{2+} and O_2 in reactor # i, respectively. Furthermore, $C^i_{\mathrm{O}_2} = \ln(\lambda u_1^i + 1)$ and λ is the coefficient of dissolved oxygen. α, β and γ are the reaction orders.

With respect to the hydrolysis reaction described in (2), ferric iron is hydrolysed to goethite, and the hydrolysis rate v_2^i of reactor # i can be computed as follows:

$$v_2^i = k_2^i c_2^i \quad i = 1, 2, 3, 4, \tag{6}$$

where k_2^i is the rate constant in reactor # i.

Regarding the neutralization reaction described in (3), hydrogen ions are neutralized by zinc oxide. The neutralization rate v_3^i of reactor # i can be computed as follows:

$$v_3^i = k_3^i u_2^i c_3^i \quad i = 1, 2, 3, 4, \tag{7}$$

where k_3^i is the rate constant in reactor # i.

As mentioned in the previous description of the goethite process and the analysis of the reaction rate, based on the law of the conservation of mass and the continuously stirred tank reactor (CSTR) model, the dynamic model of the goethite process is proposed to be the following:

$$\dot{c}^i = A_1^i c_0^i + A_2^i c^i + \phi^i(c^i, u^i) = f^i(c_0^i, c^i, u^i, t), \tag{8}$$

$$A_1^1 = \begin{bmatrix} \frac{F}{V} & 0 & 0 \\ 0 & \frac{F}{V} & 0 \\ 0 & 0 & \frac{F}{V} \end{bmatrix},$$

$$A_1^i = \begin{bmatrix} \frac{F+F_u}{V} & 0 & 0 \\ 0 & \frac{F+F_u}{V} & 0 \\ 0 & 0 & \frac{F+F_u}{V} \end{bmatrix} \quad i = 2, 3, 4,$$

$$A_2^i = \begin{bmatrix} -\frac{F+F_u}{V} & 0 & 0 \\ 0 & -\frac{F+F_u}{V} & 0 \\ 0 & 0 & -\frac{F+F_u}{V} \end{bmatrix} \quad i = 1, 2, 3, 4,$$

$$\boldsymbol{\phi}^i = \begin{bmatrix} -4v_1^i \\ 4v_1^i - v_2^i \\ -4v_1^i + 3v_2^i - 2v_3^i \end{bmatrix} \quad i = 1, 2, 3, 4,$$

where i is the reactor number, c_0^i is the inlet ion concentration in reactor # i, F and F_u are the flow rates of the leaching solution and the underflow, respectively, and V denotes the volume of the reactors. The model parameters of the goethite process adopted in this paper are shown in Table 2.

2) FORMULATION OF THE OPTIMIZATION PROBLEM FOR THE GOETHITE PROCESS

The control objective of the goethite precipitation process is to satisfy the technical requirements with minimal process consumption. Therefore, the objective function can be described as follows:

$$\min J = \sum_{i=1}^{4} \int_0^{T_f} [p_1 * u_1^i(t) + p_2 * u_2^i(t)]dt, \tag{9}$$

where T_f denotes the residence time of solution from reactor # 1 to reactor # 4, $T_f = 4V/(F+f)$, and p_1 and p_2 are the price of oxygen and zinc oxide, respectively.

In fact, there are several constraints on the optimization problem for the goethite process. First, considering the equipment capacity and production requirements in actual practice, the addition amounts of oxygen and zinc oxide should have lower and upper bounds. Second, the inlet reactant concentration of reactor # i is the outlet reactant concentration of reactor # $(i-1)$. Third, as Table 1 shows, the outlet ion concentrations should satisfy technical requirements. Integrated with an objective function and several constraints, the optimization problem for the goethite process can be described by

TABLE 3. The model parameters of the goethite process.

Parameter	reactor #1	reactor #2	reactor #3	reactor #4
k_1	1.0908e-4	0.08075	0.3208	0.4227
k_2	1.5196	4.0096	2.8096	1.7457
k_3	3.864	65.7658	35.7562	37.9162
α	2	2	2	2
β	1	1	1	1
λ	-0.36	-0.36	-0.36	-0.36

the following:

$$\min\ J = \sum_{i=1}^{4} \int_0^{T_f} [p_1 * u_1^i(t) + p_2 * u_2^i(t)]dt$$
$$\text{s.t.} \begin{cases} \dot{c}^i = f^i(c_0^i, c^i, u^i, t) & i = 1, 2, 3, 4, \\ c_0^i = c_0^{i-1}(t) & i = 1, 2, 3, 4, \\ \mathrm{u}_{1,min}^i \le \mathrm{u}_i^i(t) \le \mathrm{u}_{1,max}^i & i = 1, 2, 3, 4, \\ \mathrm{u}_{2,min}^i \le \mathrm{u}_2^i(t) \le \mathrm{u}_{2,max}^i & i = 1, 2, 3, 4, \\ c_{1,\min}^i \le c_1^i(t) \le c_{1,\max}^i & i = 1, 2, 3, 4, \\ c_2^i(t) \le c_{2,\max}^i & i = 1, 2, 3, 4, \\ c_{3,\min}^i \le c_3^i(t) \le c_{3,\max}^i & i = 1, 2, 3, 4. \end{cases} \quad (10)$$

III. MULTI-OBJECTIVE OPTIMIZATION PROBLEM BASED ON THE PID CONTROL STRATEGY FOR THE GOETHITE PROCESS

The optimization problem for the goethite process is given in the previous section. The optimization problem for the goethite process is a single objective optimization problem with several complex, nonlinear constraints. Specifically, for each reactor, the outlet ion concentrations should lie within a desired range, called state constraints, which are difficult to satisfy. To simplify the optimization difficulties caused by these state constraints, a new optimization method based on a set-point tracking strategy is proposed in this section. Based on the set-point tracking strategy, a single objective optimization problem with complex state constraints for the goethite process can be transformed into a bi-objective optimization problem. Furthermore, PID controllers are adopted to control the goethite process, and a multi-objective state transition algorithm (MOSTA) is proposed to obtain the optimal parameters of the PID controllers.

A. OPTIMIZATION METHOD BASED ON A SET-POINT TRACKING STRATEGY

The optimization method based on a set-point tracking strategy is designed for single objective optimization problems (SOPs) with complex state constraints. Although there are many ways to cope with these problems, single objective constrained optimization problems are still a difficult task [13]. In this section, an optimization method based on a set-point tracking strategy is proposed. The set-point tracking strategy is designed for single objective optimization problems that have upper and lower bounds on the state constraints of state variables. The procedures for set-point tracking strategies are as follows:

Step 1. Set proper set-points for state variables.

Step 2. Establish an objective in which the error between set-points and state variables is minimal; then, the single optimization problem with state variable constraints is converted into a bi-objective optimization problem.

Step 3. Use the state transition algorithm to solve the bi-objective problems.

The optimization method based on set-point tracking strategies converts the single objective optimization problem for the goethite process mentioned in (10) into a bi-objective optimization problem. The single objective optimization problem for the goethite process mentioned in (10) indicates that the problem has high nonlinearity and strong coupling. Moreover, the state variables (ion concentrations) and control variables (zinc oxide and oxygen addition amounts) with upper and lower bound constraints are functions of time rather than scalar quantities, which indicates that the problem is an infinite dimensional problem. The set-point tracking strategy applied to the optimization problem for the goethite process simplifies the difficulties of the problem.

According to [6], when the proportion of descent gradient in the four reactors is approximately close to (11), the goethite process will have a higher quality,

$$d_{Fe^{2+}}^1 : d_{Fe^{2+}}^2 : d_{Fe^{2+}}^3 : d_{Fe^{2+}}^4 = 4 : 3 : 2.5 : 0.5. \quad (11)$$

The set-points for the ferrous ion concentrations are set according to (11). The set-points for the ferric ion and hydrogen ion concentrations in each reactor are set to values in accordance with the production data. The set-points for the ferrous iron, ferric iron, and hydrogen ion concentrations in reactor #i are denoted by c_{1set}^i, c_{2set}^i, and c_{3set}^i, respectively. The procedures of determining the set-points for the goethite process are as follows: first, according with the inlet concentrations of ferrous ion from the production data and (11), calculate the set-points for the ferrous ion concentrations in each reactor. Then, according with the ratio of stoichiometric coefficient of chemical reaction occurring in the goethite among the ion concentrations of ferrous ion, ferric ion and hydrogen ion, the ferric ion and hydrogen ion concentrations are determined. Finally, the calculated value should be modified according to the expert knowledge. Another objective is established as follows:

$$\begin{aligned}\min J_1 = &\sum_{i=1}^{4}\int_0^{T_f}\{|c_{1set}^i - c_1^i(t)|\}dt\\ &+\sum_{i=1}^{4}\int_0^{T_f}\{|c_{2set}^i - c_1^i(t)|\}dt\\ &+\sum_{i=1}^{4}\int_0^{T_f}\{|c_{3set}^i - c_1^i(t)|\}dt. \end{aligned}\tag{12}$$

Therefore, the optimization problem for the goethite process is transformed into the bi-objective optimization problem based on set-point tracking strategy shown in (13), which is much simpler than (10).

$$\begin{cases}\min J_1 = \sum_{i=1}^{4}\int_0^{T_f}\{|c_{1set}^i - c_1^i(t)|\}dt\\ \qquad + \sum_{i=1}^{4}\int_0^{T_f}\{|c_{2set}^i - c_1^i(t)|\}dt\\ \qquad + \sum_{i=1}^{4}\int_0^{T_f}\{|c_{3set}^i - c_1^i(t)|\}dt\\ \min J_2 = \sum_{i=1}^{4}\int_0^{T_f}(p1 * u_1^i(t) + p2 * u_2^i(t))dt,\\ s.t.\ \dot{c}^i = f^i(c_0^i, c^i, u^i, t),\\ \quad c_0^i = c_0^{i-1}(t),\\ \quad \mathrm{u}_{1,min}^i \le \mathrm{u}_i^i(t) \le \mathrm{u}_{1,max}^i,\\ \quad \mathrm{u}_{2,min}^i \le \mathrm{u}_2^i(t) \le \mathrm{u}_{2,max}^i.\end{cases}\tag{13}$$

where $i \in 1, 2, 3, 4$.

The goethite process is a dynamic and nonlinear process that makes it difficult to acquire a sound control effect. Considering that proportional, integrative, and derivative (PID) controllers are among the most used in industrial control applications and given the multi-objective optimization problem for the goethite process mentioned above, we adopt PID controllers to control the goethite process. The optimal parameters of the PID controllers are obtained by MOSTA.

B. RELATED KNOWLEDGE FOR MULTI-OBJECTIVE OPTIMIZATION AND PID CONTROLLERS

Two important things are described in this section: concepts of multi-objective optimization and the structure of PID controllers.

1) BASIC CONCEPTS OF MULTI-OBJECTIVE OPTIMIZATION

There are several concepts in multi-objective optimization [11].

Definition 1 (General Multi-Objective Optimization Problem): A general multi-objective optimization problem is defined as the minimization (or maximization) of the objective function set $F(\boldsymbol{x}) = \{f_1(x), \ldots f_m(x)\}$ subject to inequality constraints $g_i(\boldsymbol{x}) \le 0$, $i = \{1, 2, \ldots\}$ and equality constraints $h_i(\boldsymbol{x}) = 0$, $i = \{1, 2, \ldots\}$, where $\boldsymbol{x}$ is an n-dimensional decision variable vector $\boldsymbol{x} = (x_1, \ldots, x_n)$ in the decision space Ω. Its peculiarity is that a solution is good for some objective functions and bad for others [14], [15]. This can be formulated as follows:

$$\begin{aligned}&\min\ F(\boldsymbol{x}) = (f_1(\boldsymbol{x}), f_2(\boldsymbol{x}), \ldots, f_m(\boldsymbol{x}))\\ &\text{s.t.}\begin{cases}g_i(\boldsymbol{x}) \le 0 & i = 1, 2, 3\ldots,\\ h_j(\boldsymbol{x}) = 0 & j = 1, 2, 3\ldots.\end{cases}\end{aligned}\tag{14}$$

Definition 2 (Pareto Dominance): A vector $\mathbf{u} = (u_1, \ldots, u_K)$ is said to dominate $\mathbf{v} = (v_1, \ldots, v_K)$ if $u_i \le v_i$ and $u_i < v_i$ for at least one $i \in I$. This is denoted by $u \succeq v$, $I = [1, 2, \ldots K]$.

Definition 3 (Pareto Optimality): With respect to the decision (variable) space Ω, a solution $\mathbf{x}^* \in \Omega$ is said to be Pareto optimal if and only if there is no $\boldsymbol{x} \in \Omega$ for which $F(\boldsymbol{x})$ dominates $F(\boldsymbol{x}^*)$.

Definition 4 (Pareto Optimal Set): For a given MOP, the Pareto optimal set P^* is defined as

$$P^* := \{\boldsymbol{x}^* | \neg\exists \boldsymbol{x} \in \Omega, F(\boldsymbol{x}^*) \preceq f(\boldsymbol{x})\}\tag{15}$$

within the decision space. Pareto optimal solutions are those solutions whose corresponding variables cannot be improved when all the objectives are considered simultaneously.

Definition 5 (Pareto Front): For a given MOP and the Pareto optimal set P^*, the Pareto front PF^*, is defined as

$$PF^* := \{u = F(\boldsymbol{x}) | \boldsymbol{x} \in P^*\}.\tag{16}$$

2) THE STRUCTURE OF THE PID CONTROLLER

The PID controller compares the measured process value with a reference set-point value. The difference or error is then processed to calculate a new process input. This input will be used to try to adjust the measured process value back to the desired set-point. The PID controller is able to manipulate the process inputs based on the history and rate of change of the signal, which can give a much more accurate and stable control method [24]–[26]. The transfer function of the PID is the following:

$$H(s) = K_p(1 + \frac{1}{T_i s} + T_d s).\tag{17}$$

The continuous form of a PID controller can be described as follows:

$$u(t) = K_p\{e(t) + \frac{1}{T_i}\int_0^t e(\sigma)d\sigma + T_d\frac{de(t)}{dt}\},\tag{18}$$

where $e(t)$ is the error signal between the set-point and the actual output of the process, and $u(t)$ is the control force. Approximate the integral and the derivative terms, the discrete form of the PID controller can be given by the following using $\int_0^t e(\sigma)d\sigma \approx T\sum_{n=0}^{N} e(k)$, $\frac{de(t)}{dt} \approx \frac{e(k)-e(k-1)}{T}$,

$$u(k) = K_p(e(k) + K_i\sum_{n=0}^{N} e(k) + K_d(e(k) - e(k-1))),\tag{19}$$

where k is the discrete step at time t, $K_i = \frac{K_p T}{T_i}$, and $K_d = \frac{K_p T_d}{T}$.

TABLE 4. The range of PID controller parameters.

Bound	K_i^i	K_p^i	K_d^i
low bound	200	0.0001	0.0001
up bound	800	5	2

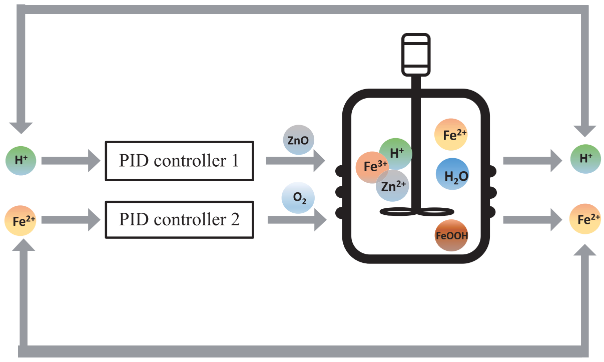

FIGURE 3. The schematic diagram of reactions in goethite process.

Furthermore, the incremental form of the PID controller can be given as follows:

$$\Delta u(k) = K_p[e(k) - e(k-1)] + K_i e(k) + K_d[e(k) - 2e(k-1) + e(k-2)]. \quad (20)$$

The relationship between u and the parameters of the PID controller can be simply described as $u(k) = g(K_p, K_i, K_d, e(k))$.

C. OPTIMIZATION PROBLEM FORMULATION

The parameters of the PID controllers determine the control performance and the concentrations of outlet ions for the goethite process. The optimization control problem for the goethite process can be transformed into an optimization problem for the parameters, which aims to find optimal parameters of the PID controllers to satisfy the technical requirements of the outlet ion concentrations. It can be concluded from the goethite process that oxygen can directly influence the ferrous ion concentration and that zinc oxide can directly influence the hydrogen ion concentration. However, the ferric ion concentration can not be changed by oxygen or zinc oxide directly. Therefore, for each reactor, two PID controllers are employed. One is employed to control the zinc oxide addition amount according to the error between the hydrogen ion concentration and its desired set concentration, and the other is employed to control the oxygen addition amount according to the error between the ferrous ion concentration and its desired set concentration. Ferric ion concentrations are controlled indirectly by oxygen and zinc oxide addition. The schematic diagram of PID control for the goethite process in each tank is shown in Fig. 3.

There are three important parts of the optimization problem for the PID controller parameters:

1. (1) Decision variables: The parameters of the PID controllers are chosen to be the decision variables of the model. Each PID has three parameters, and each reactor needs two PID controllers. Therefore, there needs to be eight PID controllers, and the dimension of the decision variables in the optimization problem is 24, which can be denoted by $K = [K^1, \ldots K^j]$, where $K^j = [K_p^j, K_i^j, K_d^j]$ and j indicates the jth PID controller with $j \in [1, 8]$.
2. (2) Objective function: As mentioned above, minimizing the first objective will provide good reference tracking, and minimizing the second reduces the quantity of oxygen and zinc oxide and thus the cost of the control.
3. (3) Constraint condition: In addition to the constraint conditions mentioned in (13), the parameters of the PID controllers have a desirable range shown in Table 4, namely,

$$\begin{aligned} K_{min,p}^j &< K_p^j < K_{max,p}^j, \\ K_{min,i}^j &< K_i^j < K_{max,i}^j, \\ K_{min,d}^j &< K_d^j < K_{max,d}^j. \end{aligned} \quad (21)$$

In summary, the bi-objective optimization problem based on PID control for the goethite process can be written as follows:

$$\begin{cases} \min\ J_1 = \sum_{i=1}^4 \int_0^{T_f} \{|c_{1set}^i - c_1^i(t)|\}dt \\ \qquad + \sum_{i=1}^4 \int_0^{T_f} \{|c_{2set}^i - c_1^i(t)|\}dt \\ \qquad + \sum_{i=1}^4 \int_0^{T_f} \{|c_{3set}^i - c_1^i(t)|\}dt, \\ \min\ J_2 = \sum_{i=1}^4 \int_0^{T_f} (p1 * u_1^i(t) + p2 * u_2^i(t))dt, \\ s.t.\ \dot{c}^i(t) = f^i(c_0^i(t), c^i(t), u^i(t)), \\ \quad c_0^i(t) = c_0^{i-1}(t), \\ \quad u_1^i(t) = g_1(c_0^{i-1}(t), K^i, c_{set}^i(t)), \\ \quad u_2^i(t) = g_2(c_0^{i-1}(t), K^i, c_{set}^i(t)), \\ \quad \mathrm{u}_{1,min}^i \le \mathrm{u}_i^i(t) \le \mathrm{u}_{1,max}^i, \\ \quad \mathrm{u}_{2,min}^i \le \mathrm{u}_2^i(t) \le \mathrm{u}_{2,max}^i, \\ \quad K_{min,p}^j < K_p^j < K_{max,p}^j, \\ \quad K_{min,i}^j < K_i^j < K_{max,i}^j, \\ \quad K_{min,d}^j < K_d^j < K_{max,d}^j. \end{cases} \quad (22)$$

where $i \in 1, 2, 3, 4$. To reveal the fact that PID control based on the set-point tracking strategy can effectively simplify the difficulty of the optimization control problem for the goethite process, single objective PID control is adopted for the sake of comparison. Focusing on several complex constraints, the penalty function method is adopted. In accordance with the technical requirements in Table 1, the optimization objective function of the single objective PID controller can be

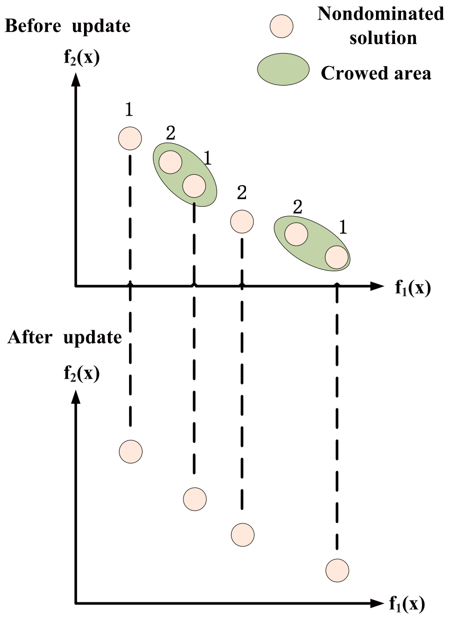

FIGURE 4. The schematic diagram of distance update operator.

TABLE 5. The parameters of MOSTA.

Parameter	value
SE	40
ε_α	1→1e-4
ε_β	1
ε_γ	1
ε_δ	1
fc	2

described as follows, where s_ι are the penalty factors and are equal to 10e3:

$$\min Q = \sum_{i=1}^{4}\sum_{k=0}^{N}(p1 * u_1^i(k) + p2 * u_2^i(k)) + \sum_{\iota=0}^{3} s_\iota G_\iota, \quad (23)$$

where

$$G_1 = \sum_{k=0}^{N}\sum_{i=1}^{4}\max(c_{1,min}^i - c_1^i, c_1^i - c_{1,max}^i, 0),$$

$$G_2 = \sum_{k=0}^{N}\sum_{i=1}^{4}\max(c_{2,min}^i - c_2^i, c_2^i - c_{2,max}^i, 0),$$

$$G_3 = \sum_{k=0}^{N}\sum_{i=1}^{4}\max(c_{3,min}^i - c_3^i, c_3^i - c_{3,max}^i, 0).$$

IV. PROPOSED MULTI-OBJECTIVE STATE TRANSITION ALGORITHM

To solve the bi-objective optimization problem for the goethite process mentioned above, a multi-objective state transition algorithm (MOSTA) is proposed. MOSTA integrates the state transition algorithm (STA) [19], [20] with

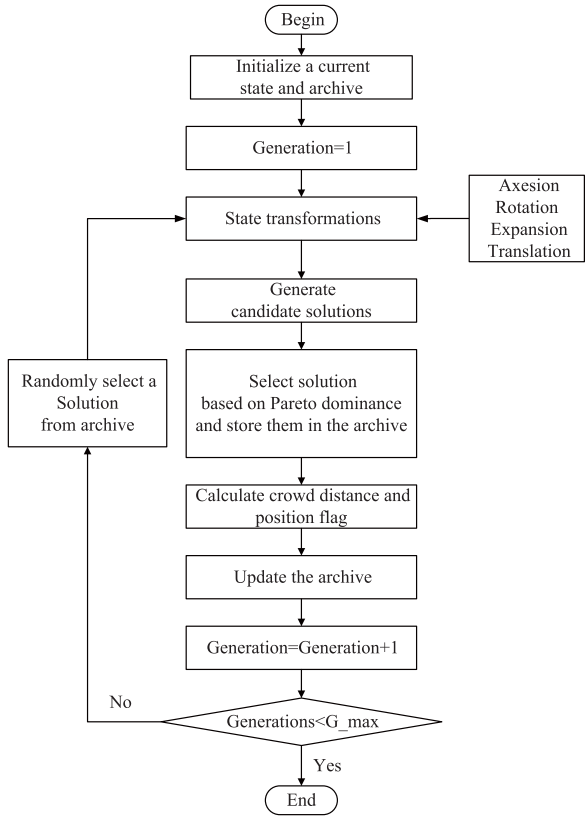

FIGURE 5. The flow chart of MOSTA.

the concept of Pareto dominance to solve multi-objective optimization problems. The nondominated individuals found along the evolutionary process are stored in the archive. By using convergence and spacing metrics for evaluation, MOSTA shows fast convergence. Solutions can approximate the true Pareto front compared with other algorithms, which indicates that the algorithm we proposed is a valid approach to solving multi-objective problems. There are three main goals in multi-objective optimization problem solving [16] : to preserve nondominated points in the objective space and associated solution points in the decision space, which is called the "search engine," to keep making algorithmic progress towards the Pareto front in the objective function space, which is called the "selection strategy," and to maintain the diversity of points on the Pareto front, which is called "diversity preservation." The description of MOSTA will pursue these goals.

A. SEARCH ENGINE OF MOSTA

Four special state transformation operators are designed to solve continuous optimization problems with single objectives [17], [18]. Because these operators present good search performance in global and local searches, these operators are adopted in MOSTA to search for Pareto optimal solutions in the feasible space. For a given solution, many different candidate solutions can be generated by the state transition operators. All the candidate solutions are generated by four operators and will be selected in the next period.

TABLE 6. Bechmark test functions of multi-objectives optimization algorithms.

problems	dimension	variable domain	objective functions
KUR	3	[-5,5]	$f_1(x) = \sum_{i=1}^{n-1} -10e^{-0.2\sqrt{x_i^2+x_{i+1}^2}}$ $f_2(x) = \sum_{i=1}^{n} \lvert x_i\rvert^{0.8} + 5\sin(x_i)^3$
ZDT1	30	[0,1]	$f_1(x) = x_1$ $f_2(x) = g(x)[1 - \sqrt{\frac{x_1}{g(x)}}]$ $g(x) = 1 + \frac{9\sum_{i=2}^{n} x_i}{(n-1)}$
ZDT2	30	[0,1]	$f_1(x) = x_1$ $f_2(x) = g(x)[1 - (\frac{x_1}{g(x)})^2]$ $g(x) = 1 + \frac{9\sum_{i=2}^{n} x_i}{(n-1)}$
ZDT3	30	[0,1]	$f_1(x) = x_1$ $f_2(x) = g(x)[1 - \sqrt{\frac{x_1}{g(x)}} - \frac{x_1}{g(x)}\sin(10\pi x_i)]$ $g(x) = 1 + \frac{9\sum_{i=2}^{n} x_i}{(n-1)}$

(1) Rotation transformation

$$x_{l+1} = x_l + \varepsilon_\alpha \frac{1}{\omega\|x_l\|_2} R_r x_l, \tag{24}$$

where ε_α is a positive constant, called the rotation factor, R_r is a random matrix with its entries being uniformly distributed random variables defined on the interval [-1, 1], and $\|\cdot\|_2$ is the 2-norm of a vector. This rotation transformation's function is to search in a hypersphere with a maximal radius.

(2) Translation transformation

$$x_{l+1} = x_l + \varepsilon_\beta R_t \frac{x_l - x_{l-1}}{\|x_l - x_{l-1}\|_2}, \tag{25}$$

where ε_β is a positive constant, called the translation factor, and R_t is a uniformly distributed random variable defined on the interval [0,1]. The translation transformation's function is to search along a line from x_{l-1} to x_l with the starting point x_l and a maximum length of ε_β.

(3) Expansion transformation

$$x_{l+1} = x_l + \varepsilon_\gamma R_e x_l, \tag{26}$$

where ε_γ is a positive constant, called the expansion factor, and R_e is a random diagonal matrix whose entries obey a Gaussian distribution. The expansion transformation's function is to expand the entries in x_l to the range $[-\infty, +\infty]$, searching the entire space.

(4) Axesion transformation

$$x_{l+1} = x_l + \varepsilon_\delta R_a x_l, \tag{27}$$

where ε_δ is a positive constant, called the axesion factor, and R_a is a random diagonal matrix whose entries obey a Gaussian distribution with only one random position having a nonzero value. The axesion transformation's aim is to search along the axes, strengthening the single dimensional search.

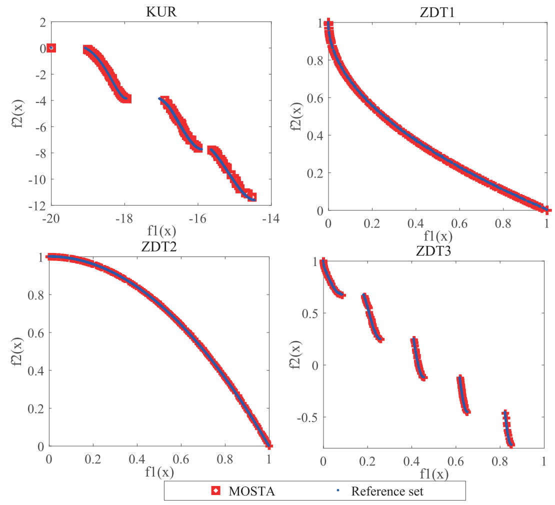

FIGURE 6. The pareto front obtained by MOSTA .

B. SELECTION STRATEGY BASED ON AN ARCHIVE

We consider the fact that a solution that is nondominated with regard to its current population is not necessarily nondominated with respect to all the candidates. Moreover, the final solution we obtain should be nondominated with regard to every other solution. Thus, an archive is used to store all the nondominated solutions. If a solution is to enter the archive, it cannot be dominated by any one solution stored in the archive. Conversely, if a solution dominates any solutions stored in the archive, the dominated solution must be removed. In this way, solutions in the archive will be the Pareto optimal solutions.

C. DIVERSITY PRESERVATION BASED ON THE EUCLIDEAN DISTANCE

A new approach without any user-defined parameters is proposed to preserve the diversity of MOSTA. The approach

TABLE 7. The mean and variance of convergence metric on benchmark functions.

Algorithm	Value	KUR	ZDT1	ZDT2	ZDT3
MOSTA	mean	4.4993e-4	1.0041e-5	**7.5117e-7**	**4.9042e-6**
	variance	0.0019	**5.4796e-7**	**3.7306e-7**	**9.0063e-7**
NSGA-II	mean	4.47764e-6	8.2049e-6	3.4319e-6	0.0248
	variance	1.4108e-6	8.8819e-7	1.7294e-6	0.0011
SPEA2	mean	0.0017	0.0140	0.0017	0.0055
	variance	0.0029	0.0071	0.0027	0.0052
PESA2	mean	0.0022	0.0305	8.8416e-5	0.0224
	variance	0.0060	0.0168	1.0697e-4	0.0106

TABLE 8. The mean and variance of spacing metric on benchmark functions.

Algorithm	Value	KUR	ZDT1	ZDT2	ZDT3
MOSTA	mean	0.1356	**0.0037**	**0.0038**	**0.0068**
	variance	0.1213	**3.5049e-4**	**3.1330e-4**	0.0012
NSGA-II	mean	0.1126	0.0073	0.0072	0.0094
	variance	0.0192	8.4093e-4	6.0694e-4	5.7832e-4
SPEA2	mean	0.5361	0.0689	0.0547	0.0605
	variance	0.4215	0.0385	0.0245	0.0361
PESA2	mean	0.2552	0.0329	0.0231	0.0741
	variance	0.0859	0.0184	0.0062	0.0611

is used to estimate the density of solutions surrounding a particular solution. There are several definitions used in this approach.

Definition 6 (Boundary Individual): Solutions with the smallest or largest value of the objective function are boundary individuals.

Definition 7 (Crowd Distance): The crowd distance of a solution that does not belong to the set of boundary individuals is the minimum value of the geometric distance between it and other solutions adjacent to it. The crowd distance of boundary individuals is assigned as inf.

$$d(i) = \min\{d(i, i-1), d(i, i+1)\}, \tag{28}$$

$$d(i, j) = \| F(i) - F(j) \|_2 \ . \tag{29}$$

Definition 8 (Position flag): A position flag is used to reflect which two individuals are relatively near. Consider these individuals, which do not belong to the set of boundary individuals: If the crowd distance $d(i) = d(i, i-1)$ of individual i, then the position flag is assigned to 1. If the crowd distance $d(i) = d(i, i+1)$ of individual i, then the position flag is assigned to 2. If the crowd distance of individual i

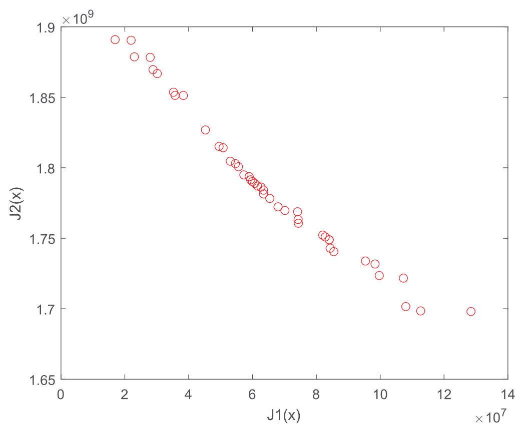

FIGURE 7. The Pareto front of PID parameters obtained MOSTA.

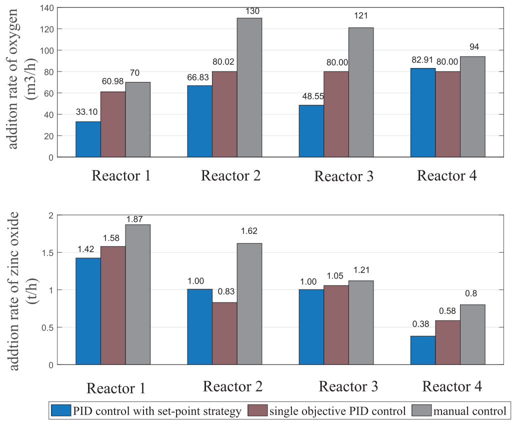

FIGURE 8. Addition rate of oxygen and zinc oxide among three method.

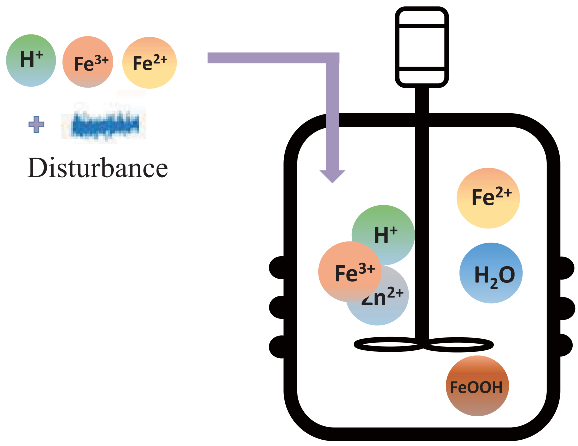

FIGURE 9. The schematic diagram of disturbance I.

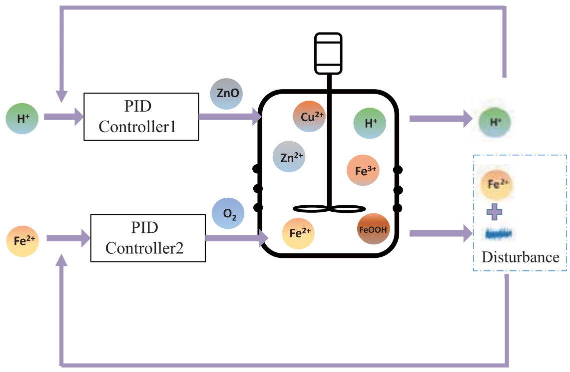

FIGURE 10. The schematic diagram of disturbance II.

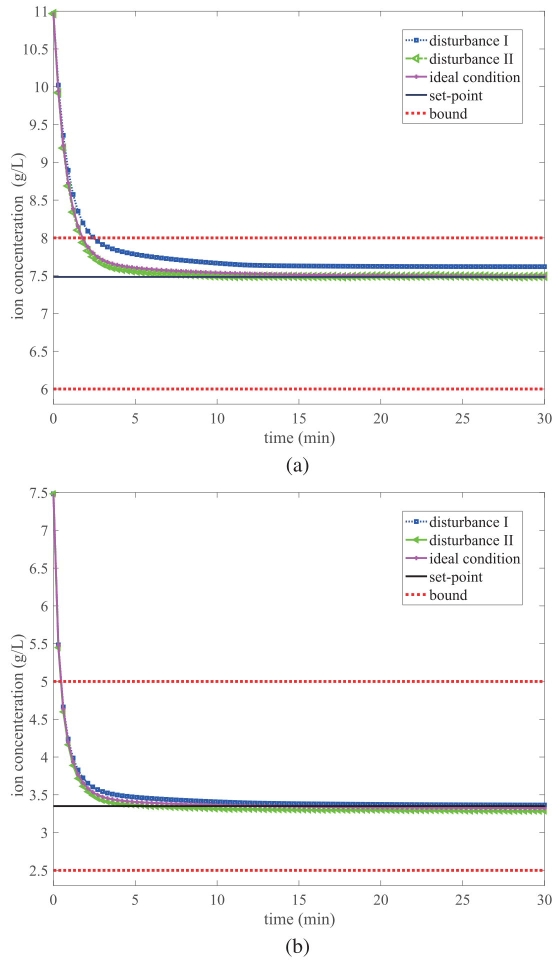

FIGURE 11. Ferrous iron ion concentration by PID control with set-point tracking strategy with disturbance (1). (a) Ferrous iron ion concentration in reactor #1. (b) Ferrous iron ion concentration in reactor #2.

is equal to 2 and the neighbour distance of individual $i+1$ is equal to 1, then individual i and individual $i+1$ are relatively near. Note that the position flag of a boundary individual is assigned as 1. The steps of the distance update operator are as follows:

Step 1. Sort individuals stored in the archive according to the first objective function value in ascending order of magnitude.

Step 2. Set the neighbour distances and position flag values of the boundary individuals.

Step 3. Calculate the neighbour distances and position flags of other intermediate individuals.

Step 4. Sort the individuals in accordance with the neighbour distance in ascending magnitude.

Step 5. If i is in the top 1/3, its position flag is 2 and the position flag of $i+1$ is 1, then remove i from the archive.

Fig. 4 is a schematic diagram of the distance update operator. The circles represent nondominated solutions stored in the archive. The number above the circle is the position flag of an individual. The individuals in the green circle indicate that the distance between them is too small. The archive is updated by the distance update operator, and solutions with good distributions are obtained.

All the main parts of MOSTA are described above. The flow chart of MOSTA is shown in Fig. 5.

D. PERFORMANCE EVALUATION FOR MOSTA

Several benchmark test problems have been constructed by previous experts to test multi-objective algorithms. In this

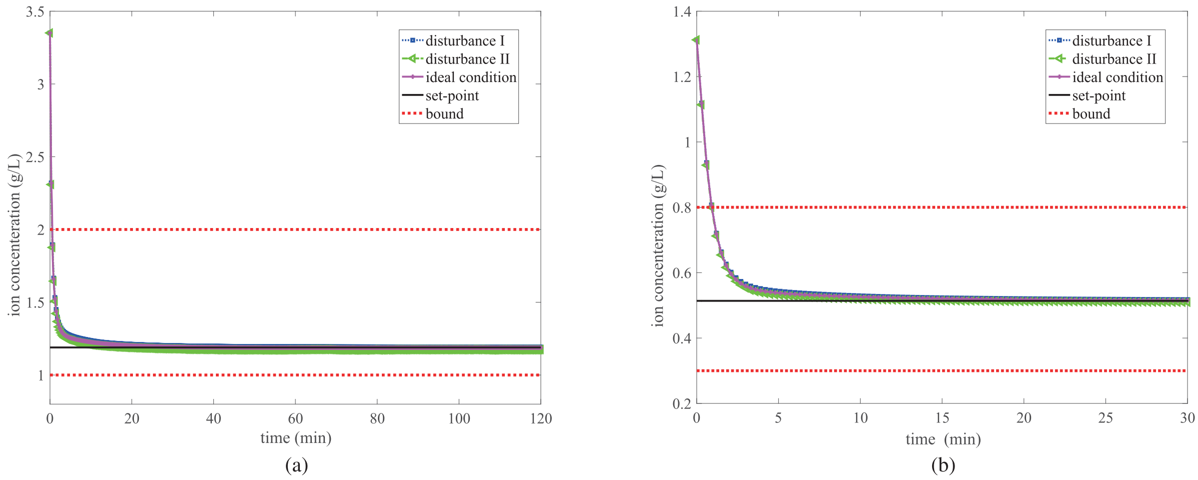

FIGURE 12. Ferrous iron ion concentration by PID control with set-point tracking strategy with disturbance (2). (a) Ferrous iron ion concentration in reactor #3. (b) Ferrous iron ion concentration in reactor #4.

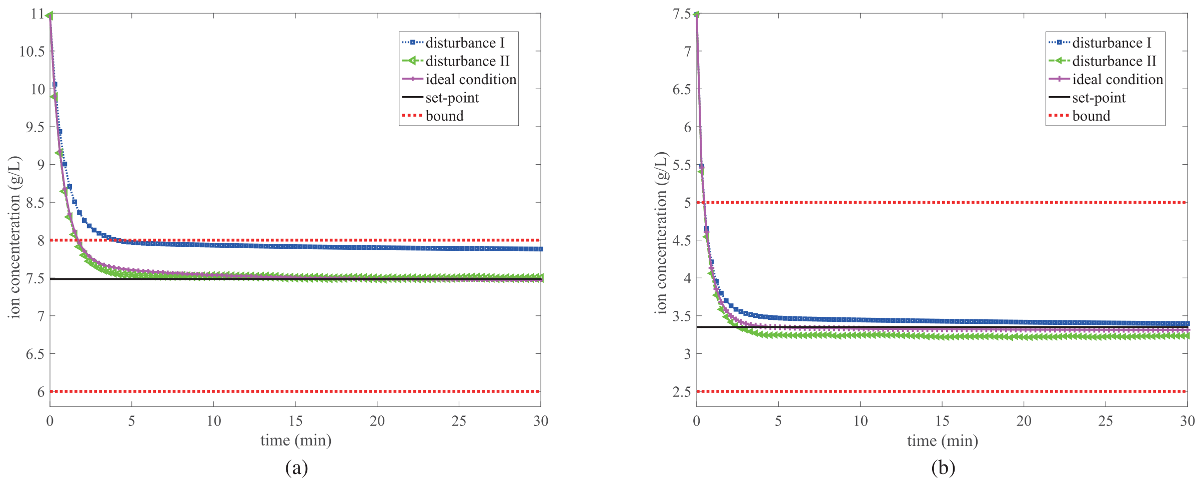

FIGURE 13. Ferrous iron ion concentration by single objective PID control with disturbance (1). (a) Ferrous iron ion concentration in reactor #1. (b) Ferrous iron ion concentration in reactor #2.

paper, four benchmark functions are chosen to verify the performance of MOSTA, which are bi-objective optimization problems with different forms of expression and properties. The parameters of MOSTA are shown in Table 5. A non-continuous function named KUR is adopted to test MOSTA. Meanwhile, three of the ZDT test problems are adopted. ZDT1 is convex functions, ZDT2 is non-convex functions, and ZDT3 is disconnected functions. The benchmark test functions are described in Table 6. The Pareto fronts of the four benchmark functions obtained by MOSTA are shown in Fig. 6.

To quantitatively analyse the convergence and diversity of MOSTA, two performance metrics are used for comparison with other classical multi-objective algorithms, NSGA-II, PESA-II and SPEA-II [21]–[23]. These are described in (30) - (32). A set $P^* = \{p_1, p_2, \ldots\}$ is defined as a reference set, which is the set of true Pareto-optimal points and the set of A=$\{a_1, a_2, \ldots\}$ is the nondominated points obtained by an algorithm.

TABLE 9. Related parameters of industrial production condition.

Parameter	Unit	Influent
pH	–	2.1
Cu^{2+}	g/L	0.03
Fe^{3+}	mol/L	0.0195
Fe^{2+}	mol/L	0.1964
Flow rate of underflow	m^3/h	49
Flow rate of leaching solution	m^3/h	150

- Convergence metric: A metric for convergence is used to evaluate convergence towards a reference set. For each point i in A, the smallest Euclidean distance to P^* can be computed as follows:

$$d_i = \min_{j=1}^{|P^*|} \sqrt{\sum_{m=1}^{N} (\frac{f_m(a_i) - f_m(p_j)}{f_m^{max} - f_m^{min}})^2}, \tag{30}$$

where f_m^{max} is the maximum and f_m^{min} is minimum of the k-th value of the objective function in reference set P^*. Then, the average of the normalized distance is computed for all points in A, and the convergence metric can be obtained,

$$C(A) = \frac{\sum_{i=1}^{|A|} d_i}{|A|}. \quad (31)$$

Thus, its value is nearly zero if the solutions are well convergent.

- Spacing metric: The value of the spacing metric reflects the distribution of solutions throughout the reference set, which is proposed to evaluate the range variance of neighbouring vectors in the reference set. A value of the spacing metric close to zero means that the solutions are well distributed. |A| is the number of the solutions obtained by the algorithm. The definition of the spacing metric is given as follows:

$$S(A) \triangleq \sqrt{\frac{\sum_{i=1}^{N} (d_{average} - d_i)^2}{|A| - 1}}, \quad (32)$$

where

$$d_i = \min \sum_{m=1}^{N} |f_m(a_i) - f_m(a_j)|$$

for $a_i, a_j \in A, i, j = 1, 2, \ldots |A|$, and

$$d_{average} = \frac{\sum_{m=1}^{|A|} d_i}{|A|}. \quad (33)$$

Table 7 and Table 8 show the comparison results for algorithms on the four benchmark test functions using the above metrics. The values of the algorithms on the four benchmark test functions for the convergence metric are less than 1e-3, which means that MOSTA can approximate the true Pareto front very well. It can be seen that the mean values of MOSTA, with respect to the convergence value on the ZDT2 and ZDT3 benchmark test functions, are much smaller than those of other algorithms. Meanwhile, the spacing metric values of performance on ZDT1 to ZDT3 for MOSTA are better than those for other algorithms, which indicates that MOSTA has a better distribution. In other words, MOSTA is a valid algorithm for solving multi-objective problems.

V. SIMULATION AND RESULTS FOR GOETHITE PRECIPITATE PROCESS

In this section, a goethite process in a zinc hydrometallurgy plant in China is investigated, and some industrial data from July 2016 are collected for analysis. Under the same industrial production conditions, including the same leaching solution, underflow and inlet ion concentration flow rates, several comparison experiments are conducted. Related parameters of industrial production conditions for the goethite precipitation process are shown in Table 9. Two kinds of optimal models based on PID control mentioned in (22) and (23) are solved,

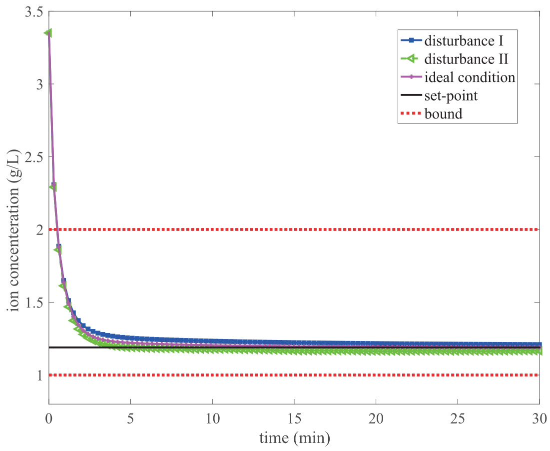

(a)

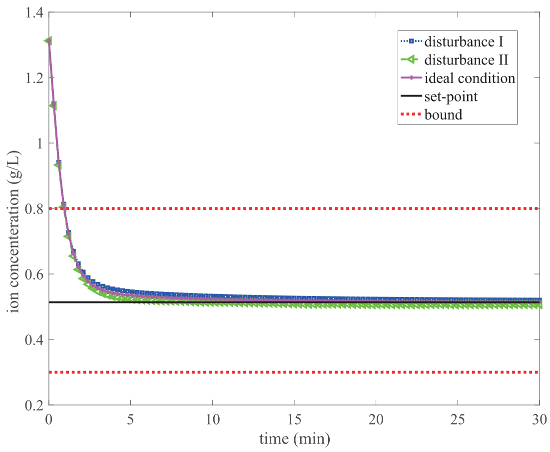

(b)

FIGURE 14. **Ferrous iron ion concentration by single objective PID control with disturbance (2). (a) Ferrous iron ion concentration in reactor #3. (b) Ferrous iron ion concentration in reactor #4.**

and two series of PID parameters are obtained. Taking into account the industrial production conditions and the ideal ferrous iron ion descent gradient mentioned in (11), the set-points of the PID controllers are shown in Table 10.

To illustrate the effectiveness of the set-point tracking strategy, two series of PID parameters are compared: (1) the solution of (22) based on the set-point tracking strategy obtained by MOSTA with minimal energy consumption, shown in Table 11, and (2) the solution of (23) obtained by STA, shown in Table 12. Several comparison experiments are conducted among PID control based on the set-point tracking strategy, PID control without the set-point tracking strategy and manual control. The addition rates of zinc oxide and oxygen are compared under these three control approaches in Fig. 8. The results show that the PID control method based on the set-point tracking strategy is a valid approach to controlling the goethite process.

Furthermore, considering that in the actual industrial process, the influence of the last working procedure of hydrometallurgical extraction of zinc on the inlet concentration of the first reactor in the goethite process and the measure-

TABLE 10. The set-points of PID controllers for the goethite process.

Set-points ion	Unit	#1 Effluent	#2 Effluent	#3 Effluent	#4 Effluent
H^+	mol/L	0.001	7.94e-4	7.94e-4	7.87e-4
Fe^{2+}	mol/L	0.1340	0.060	0.0235	0.010

TABLE 11. The parameters of PID controller with set-point tracking strategy.

Reactor	PID	K_p	K_i	K_d
#1 reactor	PID1	200	3.6391	0.5939
	PID2	200	1.9911	1.200e-4
#2 reactor	PID1	283.1798	1e-4	1e-4
	PID2	200.1900	0.6067	1.200e-4
#3 reactor	PID1	305.6134	0.8581	1.000e-4
	PID2	200.1939	0.6622	1.200e-4
#4 reactor	PID1	487.6502	0.8473	1.000e-4
	PID2	200.1720	1.9234	1

TABLE 12. The parameter of PID by single objective optimization.

Reactor	PID	K_p	K_i	K_d
#1 reactor	PID1	344.5615	4.5440	1.621e-4
	PID2	800	1.0168	1.295e-4
#2 reactor	PID1	800	1.5207	0.759
	PID2	100	1.0168	1.295e-4
#3 reactor	PID1	200	3.1643e-4	2.655e-4
	PID2	200	1.1680	2.295e-4
#4 reactor	PID1	228.2916	0.0025	3.907e-4
	PID2	200	1.1680	2.295e-4

ment noise for the outlet ion concentration may lead to a degradation of control performance, the effects of the above disturbances are taken into account to test the reliability of PID parameters. Gaussian noise with a standard deviation of $\pm 7\%$ is introduced into the inlet and outlet ion concentrations to simulate the disturbances. The noise added into the inlet ion concentration to simulate the influence of a previous work procedure is called disturbance I, which is briefly described in Fig. 9. The noise added into the outlet ion concentration to simulate the measurement is called disturbance II, which is briefly described in Fig. 10.

Comparison experiments between the disturbance and ideal conditions of the two series of PID parameters are conducted. The results of the outlet ferrous iron trends of reactor # 1 to reactor # 4 under different conditions are shown in Fig. 11 – Fig. 14. It can be seen that the ion concentrations can be stable at the set-point ion concentrations using the PID parameters obtained based on the method we proposed under both disturbance and ideal conditions. The trend of the hydrogen ion concentration without noise is shown in Fig. 15(a) and Fig. 15(b). The pH value of the four reactors satisfies industrial requirements and can be stable at the desired level.

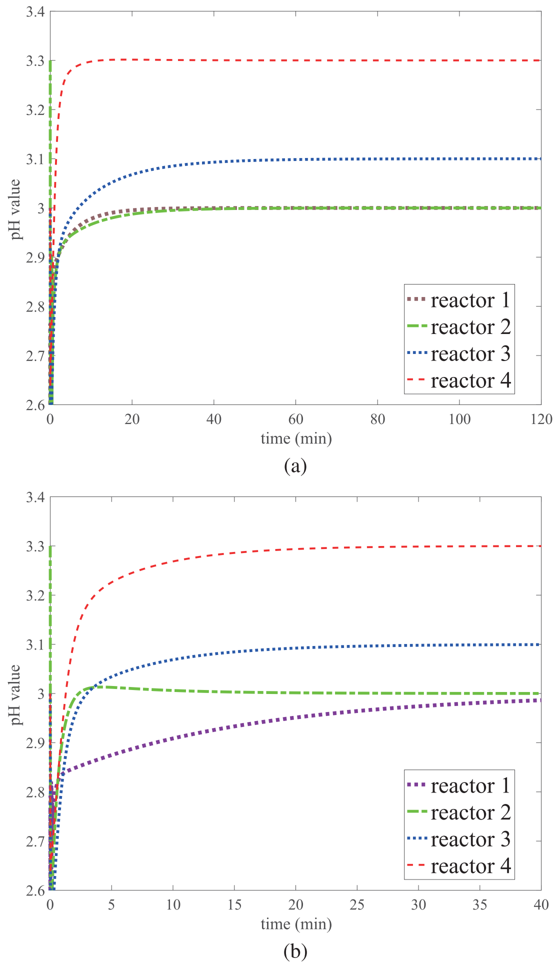

FIGURE 15. **The comparison results of pH value trend beween PID control with set-point tracking strategy and single objective PID control. (a) The pH value trend by PID control with set-point tracking strategy. (b) The pH value trend by single PID control.**

On the whole, under the proposed PID control method, the ion concentrations can satisfy production requirements with less consumption. Meanwhile, the PID parameters have the ability to reject disturbances.

VI. CONCLUSION

This paper gives a comprehensive analysis of the goethite process based on chemical kinetics. Considering complex state constraints in the goethite process, PID controllers based on a set-point tracking strategy are adopted to control the process. The set-point tracking strategy is used to transform the single objective optimization problem with complex state constraints into a bi-objective optimization problem. A multi-objective state transition algorithm (MOSTA) is designed for finding the optimal parameters of the PID controllers. Compared with PID control without the set-point tracking strategy and manual control, the proposed method has more advantages. The outlet of the ion concentrations can satisfy production requirements with less consumption, and disturbances can be rejected. Moreover, as verified by several benchmark test functions, MOSTA can approximate the true Pareto front and has a relatively high convergence precision, which indicates that it can be applied to more complex industrial practices.

REFERENCES

[1] J. C. Balarini, L. D. O. Polli, T. L. S. Miranda, R. M. Z. de Castro, and A. Salum, "Importance of roasted sulphide concentrates characterization in the hydrometallurgical extraction of zinc," *Minerals Eng.*, vol. 21, no. 1, pp. 100–110, Jan. 2008.

[2] Y. G. Li, W. H. Gui, K. L. Teo, H. Q. Zhu, and Q. Q. Chai, "Optimal control for zinc solution purification based on interacting CSTR models," *J. Process Control*, vol. 22, no. 10, pp. 1878–1889, Dec. 2012.

[3] A. Pappu, M. Saxena, and S. R. Asolekar, "Jarosite characteristics and its utilisation potentials," *Sci. Total Environ.*, vol. 59, nos. 1–3, pp. 232–243, Apr. 2006.

[4] M. R. C. Ismael and J. M. R. Carvalho, "Iron recovery from sulphate leach liquors in zinc hydrometallurgy," *Minerals Eng.*, vol. 16, no. 1, pp. 31–39, Jan. 2003.

[5] E. Güler and A. Seyrankaya, "Precipitation of impurity ions from zinc leach solutions with high iron contents—A special emphasis on cobalt precipitation," *Hydrometallurgy*, vol. 164, pp. 118–124, Sep. 2016.

[6] Y.-F. Xie, S.-W. Xie, Y.-G. Li, and W. H. Gui, "Dynamic modeling and optimal control of goethite process based on the rate-controlling step," *Control Eng. Pract.*, vol. 58, pp. 54–65, Jan. 2017.

[7] Y. Chang, X. Zhai, B. Li, and Y. Fu, "Removal of iron from acidic leach liquor of lateritic nickel ore by goethite precipitate," *Hydrometallurgy*, vol. 101, nos. 1–2, pp. 84–87, Feb. 2010.

[8] Y. Xie, S. Xie, X. Chen, W. Gui, L. Caccetta, and C. Yang, "An integrated predictive model with an on-line updating strategy for iron precipitation in zinc hydrometallurgy," *Hydrometallurgy*, vol. 151, pp. 62–72, Jan. 2015.

[9] S.-W. Xie, Y.-F. Xie, Y.-G. Li, C. Yang, and W.-H. Gui, "Optimal control of oxidizing rate for iron precipitation process in zinc hydrometallurgy," *Acta Automatica Sinica*, vol. 41, no. 12, pp. 2036–2046, Dec. 2015.

[10] J. Han, C. Yang, X. Zhou, and W. Gui, "Dynamic multi-objective optimization arising in iron precipitation of zinc hydrometallurgy," *Hydrometallurgy*, vol. 173, pp. 134–148, Nov. 2017.

[11] S.-Z. Zhao, M. W. Iruthayarajan, S. Baskar, and P. N. Suganthan, "Multi-objective robust PID controller tuning using two lbests multi-objective particle swarm optimization," *Inf. Sci.*, vol. 181, no. 16, pp. 3323–3335, Aug. 2011.

[12] W. He, T. Meng, D. Huang, and X. Li, "Adaptive boundary iterative learning control for an Euler–Bernoulli beam system with input constraint," *IEEE Trans. Neural Netw. Learn. Syst.*, vol. 29, no. 5, pp. 1539–1549, May 2018.

[13] J. Han, C. Yang, X. Zhou, and W. Gui, "A two-stage state transition algorithm for constrained engineering optimization problems," *Int. J. Control Autom. Syst.*, vol. 16, no. 2, pp. 522–534, Apr. 2018.

[14] M. Reyes-sierra and C. A. C. Coello, "Multi-objective particle swarm optimizers: A survey of the state-of-the-art," *Int. J. Comput. Intell. Res.*, vol. 2, no. 3, pp. 1051–1056, 2002.

[15] A. Zhou, B.-Y. Qu, H. Li, S.-Z. Zhao, P. N. Suganthan, and Q. Zhang, "Multiobjective evolutionary algorithms: A survey of the state of the art," *Swarm Evol. Comput.*, vol. 1, no. 1, pp. 32–49, 2011.

[16] G. Chiandussi, M. Codegone, S. Ferrero, and F. E. Varesio, "Comparison of multi-objective optimization methodologies for engineering applications," *Comput. Math. Appl.*, vol. 63, no. 5, pp. 912–942, Mar. 2012.

[17] X. Zhou, P. Shi, C.-C. Lim, C. H. Yang, and W. Gui, "A dynamic state transition algorithm with application to sensor network localization," *Neurocomputing*, vol. 273, no. 17, pp. 237–250, Jan. 2018.

[18] J. Han, C. Yang, X. Zhou, and W. Gui, "A new multi-threshold image segmentation approach using state transition algorithm," *Appl. Math. Model.*, vol. 44, pp. 588–601, Apr. 2017.

[19] Z. K. Huang, C. Yang, X. Zhou, and W. Gui, "A novel cognitively inspired state transition algorithm for solving the linear bi-level programming problem," *Cognit. Comput.*, vol. 1, pp. 1–11, May 2018.

[20] X. Zhou, C. Yang, and W. Gui, "State transition algorithm," *J. Ind. Manage. Optim.*, vol. 8, no. 4, pp. 1039–1056, Nov. 2012.

[21] K. Deb, A. Pratap, S. Agarwal, and T. Meyarivan, "A fast and elitist multiobjective genetic algorithm: NSGA-II," *IEEE Trans. Evol. Comput.*, vol. 6, no. 2, pp. 182–197, Apr. 2002.

[22] A. M. Adham, N. Mohd-Ghazali, and R. Ahmad, "Performance optimization of a microchannel heat sink using the Improved Strength Pareto Evolutionary Algorithm (SPEA2)," *J. Eng. Thermophys.*, vol. 24, no. 1, pp. 86–100, Jan. 2015.
[23] D. W. Corne, N. R. Jerram, J. D. Knowles, and M. J. Oates, "PESA-II: Region-based selection in evolutionary multiobjective optimization," in *Proc. 3rd Annu. Conf. Genetic Evol. Comput.*, 2001, pp. 283–290.
[24] K. H. Ang, G. Chong, and Y. Li, "PID control system analysis, design, and technology," *IEEE Trans. Control Syst. Technol.*, vol. 13, no. 4, pp. 559–576, Jul. 2005.
[25] H. Freire, P. B. M. Oliveira, and E. J. S. Pires, "From single to many-objective PID controller design using particle swarm optimization," *Int. J. Control, Autom. Syst.*, vol. 5, no. 2, pp. 918–932, Apr. 2017.
[26] Z. Chen, Y. Yuan, X. Yuan, Y. Huang, X. Li, and W. Li, "Application of multi-objective controller to optimal tuning of PID gains for a hydraulic turbine regulating system using adaptive grid particle swam optimization," *ISA Trans.*, vol. 56, pp. 173–187, May 2015.

XIAOJUN ZHOU received the bachelor's degree in automation from Central South University, Changsha, China, in 2009, and the Ph.D. degree in applied mathematics from Federation University Australia in 2014.

He is currently an Associate Professor with Central South University. His main interests include the modeling, optimization, and control of complex industrial process, optimization theory and algorithms, state transition algorithm, and duality theory and their applications.

JIAJIA ZHOU received the bachelor's degree in automation from Central South University, Changsha, China, in 2016, where she is currently pursuing the master's degree. Her main interests include multi-objective optimization, state transition algorithm, and the optimization and control of complex industrial process.

CHUNHUA YANG received the M.S. degree in automatic control engineering and the Ph.D. degree in control science and engineering from Central South University, Changsha, China, in 1988 and 2002, respectively.

From 1999 to 2001, she was a Visiting Professor with KU Leuven, Leuven, Belgium. Since 1999, she has been a Full Professor with the School of Information Science and Engineering, Central South University. From 2009 to 2010, she was a Senior Visiting Scholar with the University of Western Ontario, London, Canada. Her current research interests include the modeling and optimal control of complex industrial process, fault diagnosis, and intelligent control systems.

WEIHUA GUI received the B.Eng. degree in automatic control engineering and the M.Eng. degree in control science and engineering from Central South University, Changsha, China, in 1976 and 1981, respectively.

From 1986 to 1988, he was a Visiting Scholar with the University of Duisburg-Essen, Germany. He has been a Full Professor with the School of Information Science and Engineering, Central South University, since 1991. He is currently a member of the Chinese Academy of Engineering. His main research interests are the modeling and optimal control of complex industrial process, distributed robust control, and fault diagnoses.